Multimodality imaging to guide cardiac interventional procedures
Tops, L.F.
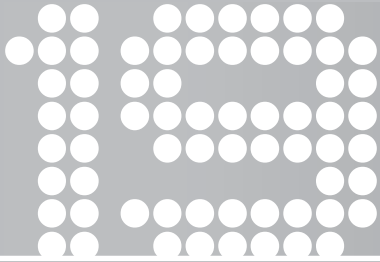
Assessment of mitral valve anatomy and geometry with 64-slice multi-slice computed tomography

Victoria Delgado[1]
Laurens F. Tops[1]
Joanne D. Schuijf[1]
Albert de Roos[2]
Josep Brugada[3]
Martin J. Schalij[1]
James D. Thomas[4]
Jeroen J. Bax[1]

[1]Department of Cardiology, Leiden University Medical Center, Leiden, the Netherlands
[2]Department of Radiology, Leiden University Medical Center, Leiden, the Netherlands
[3]Thorax Institute, Hospital Clinic, Barcelona, Spain
[4]Department of Cardiovascular Medicine, the Cleveland Clinic Foundation, Cleveland, USA

ABSTRACT

Background: By providing detailed anatomical information, MSCT may give more insight into the underlying mechanisms of functional mitral regurgitation (FMR).

Objectives: The purpose of the present study was to assess the anatomy and the geometry of the mitral valve by using 64-slice multi-slice computed tomography (MSCT).

Methods: In 151 patients, including 67 patients with heart failure (HF) and 29 patients with moderate to severe FMR, 64-slice MSCT coronary angiography was performed. The anatomy of the subvalvular apparatus of the mitral valve was assessed, and mitral valve geometry, comprising the mitral valve tenting height and leaflet tethering, was evaluated at the anterolateral, central and posteromedial levels.

Results: In the majority of patients, the anatomy of the subvalvular apparatus was highly variable due to multiple anatomic variations of the posterior papillary muscle: the anterior PM had a single insertion, whereas the posterior PM showed multiple heads and insertions (n=114, 83%). The assessment of mitral valve geometry demonstrated that HF patients with moderate to severe FMR had significantly increased posterior leaflet angle and mitral valve tenting height at the central ($44.4 \pm 11.9°$ vs. $37.1 \pm 9.0°$, p=0.008; 6.6 ± 1.4 mm/m^2 vs. 5.3 ± 1.3 mm/m^2, p<0.0001, respectively) and posteromedial levels ($35.9 \pm 10.6°$ vs. $26.8 \pm 10.1°$, p=0.04; 5.4 ± 1.6 mm/m^2 vs. 4.1 ± 1.2 mm/m^2, p<0.0001, respectively), as compared to HF patients without FMR. In addition, a more outward displacement of the PMs, reflected by a higher mitral valve sphericity index, was observed in HF patients with FMR (1.4 ± 0.3 vs. 1.2 ± 0.3, p=0.004). Mitral valve tenting height at the central level and mitral valve sphericity index were the strongest determinants of FMR severity.

Conclusions: MSCT provides anatomical and geometric information on the mitral valve apparatus. In HF patients with moderate to severe FMR, a more pronounced tethering of the mitral leaflets at the central and posteromedial levels was demonstrated using MSCT.

INTRODUCTION

Functional mitral regurgitation (FMR) is associated with poor outcome in patients with coronary artery disease and left ventricular (LV) dysfunction (1-3). One of the characteristics of FMR, different from organic mitral regurgitation, is the preserved anatomy of the leaflets and tendinous cords. Accordingly, mitral valve repair is a suitable surgical procedure to treat FMR. However, the results still remain controversial (4-7). The complex pathophysiology of FMR makes this entity a challenge for surgery. Several underlying mechanisms may contribute to FMR: LV remodeling, wall motion abnormalities, displacement of the papillary muscles (PMs) or mitral annulus deformation (8). All these mechanisms result in tethering of the mitral valve with failure of anteroposterior leaflet coaptation.

Recent advances in 3-dimensional imaging techniques have allowed for a better understanding of the aforementioned changes in the mitral valve apparatus and LV geometry (9,10). Subsequently, new strategies for surgical mitral valve repair have been proposed (11,12). Multi-slice computed tomography (MSCT) may be a valuable technique to study both LV geometry and mitral valve anatomy and geometry. Therefore, the purpose of the present study was to assess the anatomy and geometry of the mitral valve and the LV with the use of 64-slice MSCT in a large cohort of patients, including patients with FMR.

METHODS

Study population

A total of 151 consecutive patients referred to Leiden University Medical Center (Leiden, The Netherlands) for MSCT coronary angiography were studied. The study population was divided into 2 groups: group I (control patients, n = 84) comprised patients without coronary artery disease or structural heart disease and group II (heart failure-patients [HF], n = 67) comprised patients with heart failure and documented LV systolic dysfunction. The anatomy and geometry of the mitral valve were examined, and differences among the two patient groups were assessed. In addition, differences in mitral valve geometry between HF patients with and without moderate to severe FMR were assessed.

Multi-slice computed tomography

All patients underwent scanning on a 64-slice MSCT scanner (Aquilion, Toshiba Medical Systems, Tokyo, Japan) using the following protocol: 120 kV, 300 mA, a rotation time of 400 to 500 ms (depending on the heart rate), and collimation of 64 x 0.5 mm. A total of 80 to 110 ml of nonionic contrast medium (Iomeron 400, Bracco, Altana Pharma, Konstanz, Germany) was administered in the antecubital vein at 5 mL/s. Automated peak enhancement detection in the descending aorta was used to time the contrast bolus. Data acquisition started automatically

after the threshold level of +100 Hounsfield units was reached, and it was performed during an inspiratory breath-hold of 8 to 10 seconds. The ECG was recorded simultaneously to allow retrospective gating and reconstruction of the data at desired phases of the cardiac cycle. Data acquisition was performed at a rotation time of 400 ms resulting in a temporal resolution of 200 ms in case of half reconstruction. In those patients with a heart rate > 70 beats/s, 3 cardiac beats were acquired resulting in segment reconstruction algorithm with slightly lower temporal reconstruction. All images were transferred to a dedicated workstation for data analysis (Vitrea 2, Vitral Images, Plymouth, Minnesota).

Data analysis

To study the anatomy and geometry of the mitral valve and the LV, the data set was reconstructed with a slice thickness of 0.5 mm and a reconstruction interval of 0.3 mm, at 30% and 75% of the RR interval for the systolic and diastolic phases, respectively. Standard orthogonal planes were used to assess the anatomy of the mitral valve apparatus. A reconstructed LV short-axis view was used to assess the mitral valve geometry. All parameters were corrected for body surface area.

Anatomy of the subvalvular apparatus Reconstructed long-axis 2- and 4-chamber views and the reconstructed LV short-axis view in the diastolic phase were used to study the anatomy of the subvalvular apparatus. The anatomy of the PMs was assessed focusing on the number of heads (ranging from I to III) and the type of insertion to the ventricular wall (type A-C), according to the classification of morphological variants of the PMs, as described by Berdajs et al. (13) (Figure 1). Furthermore, the attachment of the basal part of the PMs to the LV wall was studied, with special attention to the type of attachment (solid or trabecularized attachment, Figure 1).
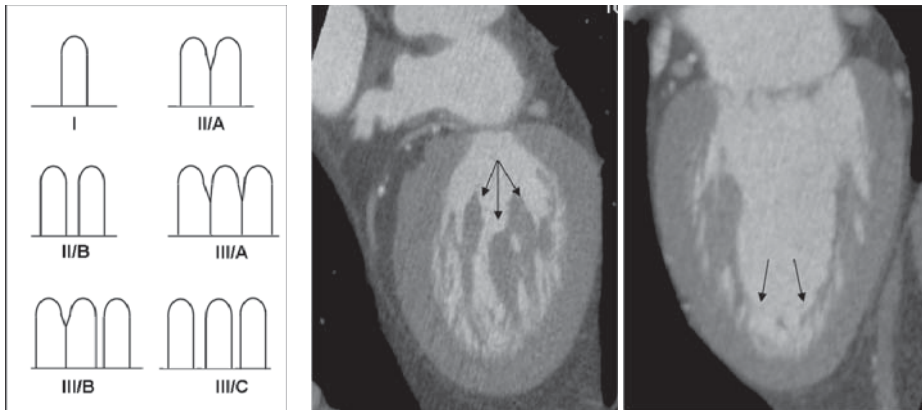
Figure 1. Assessment of subvalvular apparatus of the mitral valve. Left panel: the anatomical variations of the papillary muscles (PMs) were classified according to the number of heads and insertions (modified after Berdajs et al, reference #13). The number of PM heads could range from 1 to 3 (type I, II and III, respectively), and the insertions could be common (subtype A) or divided (subtype B or C). Middle panel: Example of a type III/B posterior PM, demonstrating 3 PM heads, with 2 insertions. Right panel: The attachment of 2 type I PM showed thin trabeculae upholstering the surface of the LV wall.

Left ventricular geometry To assess LV volumes and systolic function, the data set was reconstructed with a slice thickness of 5.0 mm in the short-axis view, starting at early systole (0% of cardiac cycle) to end-diastole (95% of cardiac cycle) in steps of 5%. Endocardial borders were traced manually on the short-axis cine images and the PMs were regarded as being part of the LV cavity. Table 1 summarizes the LV parameters that were evaluated. The LV end-diastolic volume (LVEDV) and end-systolic volume (LVESV) were obtained and the LV ejection fraction (LVEF) was calculated by the difference between LVESV and LVEDV divided by the LVEDV (Table 1). The sphericity index of the LV was calculated with the use of the following equation: LV sphericity index = EDV / [(LAD^3 x 3.14)/ 6], where LAD is the long axis diameter of the LV (14).

**Table 1.** Summary of the left ventricular and mitral valve variables

Left ventricle
LV end-diastolic volume index
LV end-systolic volume index
LV ejection fraction
LV sphericity index
Mitral valve
Mitral annulus area
Intercommisural diameter (CC diameter)
Anteroposterior diameter (AP diameter)
Mitral valve sphericity index
Distance between heads of papillary muscles
Anterior leaflet angle (Aα)
Posterior leaflet angle (Pα)
Tenting height (MVTHt)

LV = left ventricular.

Mitral valve geometry The mitral valve geometry was assessed in the reconstructed systolic phase. An overview of the measured variables is shown in Table 1. With the use of 2- and 4-chamber views and the reconstructed LV short-axis view, a plane parallel to the mitral valve was reconstructed (Figure 2). At the level of the mitral valve annulus, the mitral annulus area was calculated by planimetry and the anteroposterior diameter (AP diameter) and the inter-commissural diameter (CC diameter) were measured (Figure 2).

Subsequently, a second plane parallel to the mitral valve was reconstructed, which clearly visualized both mitral commissures. Three anteroposterior planes perpendicular to this plane were defined to assess the geometry of the anterolateral, central and posteromedial parts of the mitral leaflets (Figure 3). In all 3 planes, the degree of leaflet tethering was assessed by measuring the angle at which each leaflet met the mitral annulus plane (anterior leaflet, Aα; posterior leaflet, Pα; Figure 3). Mitral valve tenting height, defined as the distance between the leaflet coaptation and the mitral annulus plane, was also measured in all 3 planes (Figure 3) (9). Finally, in the systolic phase, the distance between the heads of PMs was measured (Figure 4).

As an estimate of PMs displacement, the sphericity index of the mitral valve was calculated (9). The mitral valve sphericity index was defined as the ratio between the distance at the level of the basis of the PMs and the distance between this level and the mitral annulus plane (Figure 5).
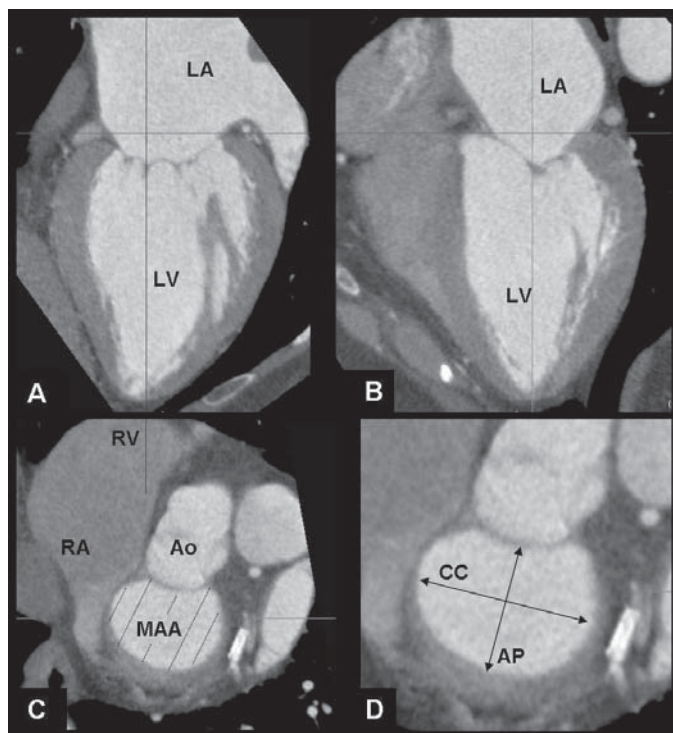
Figure 2. Assessment of the mitral valve annulus geometry. From the 2-and 4-chamber views (panel A and B), a short-axis view at the level of the mitral annulus was reconstructed (panel C).The area of the mitral annulus was quantified by planimetry. In addition, the intercommissural diameter (CC diameter) and the anteroposterior diameter (AP diameter) of the mitral annulus were assessed (panel D). Ao = aorta; LA = left atrium; LV = left ventricle; MAA = mitral annulus area; RA = right atrium; RV = right ventricle.

Echocardiography

Standard 2-dimensional echocardiograms were performed with patients in the left lateral decubitus position with a commercially available ultrasound system (Vingmed Vivid 7, General Electric-Vingmed, Milwaukee, Wisconsin). Images were obtained with a 3.5-MHz transducer at a depth of 16 cm in the parasternal (long- and short-axis) and apical (2- and 4-chamber) views. Standard 2-dimensional gray-scale images and color Doppler data were digitally stored in cine-loop format. LVEF was calculated from apical 2- and 4-chamber views with the biplane Simpson's rule (15). The severity of mitral regurgitation was graded quantitatively from color-flow Doppler in the conventional parasternal long-axis and apical 4-chamber views, using the proximal isovelocity surface area method. Effective regurgitant orifice area and regurgitant volume were calculated and mitral regurgitation was characterized according to the ACC/ AHA guidelines: mild (regurgitant orifice area <0.2 cm^2 and regurgitant volume < 30 ml/beat); moderate (regurgitant orifice area 0.2-0.39 cm^2 and regurgitant volume 30-59 ml/beat); severe (regurgitant orifice area ≥40 cm^2 and regurgitant volume ≥60 ml/beat) (16).
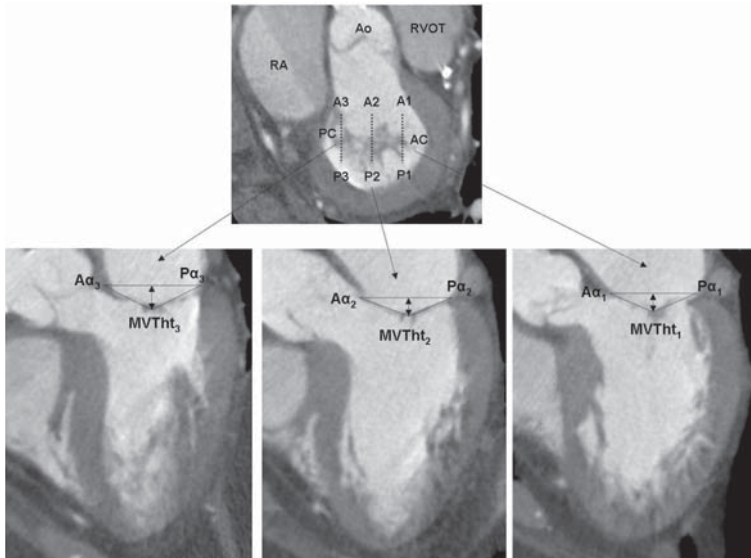
Figure 3. Assessment of the mitral valve geometry. Three anteroposterior planes perpendicular to the reconstructed LV short-axis view, at the level of the mitral commissures, were defined to assess the geometry of the anterolateral (A1-P1), central (A2-P2) and posteromedial (A3-P3) parts of the mitral leaflets. The leaflet angles (Aα and Pα, as a reflection of tenting of the leaflets) and the mitral valve tenting height were measured in all 3 planes. AC = anterior commissure; Aα = anterior leaflet angle; MVTht = mitral valve tenting height; PC = posterior commissure; Pα = posterior leaflet angle; RA = right atrium; RVOT = right ventricular outflow tract.

Figure 4. Displacement of papillary muscles. At the reconstructed systolic phase, the distance between the heads of the papillary muscles was measured, as indicated by the black arrow.
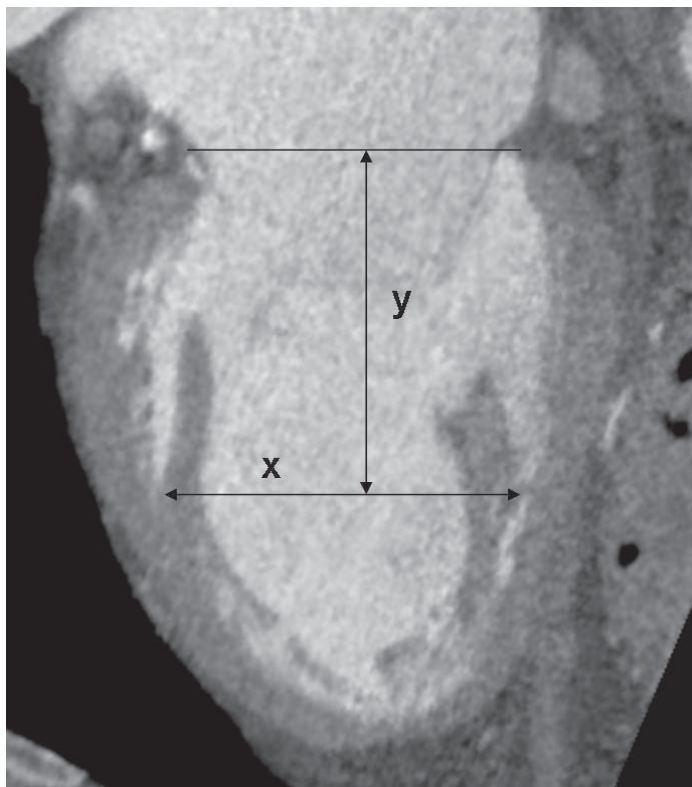
Figure 5. Sphericity index of the mitral valve. The sphericity index of the mitral valve was calculated as the ratio between the distance at the level of the papillary muscles basis (x) and the distance between this level and the mitral annulus plane (y).

Statistical analysis

Continuous variables are presented as mean values ± SD; categorical variables are presented as frequencies and percentages. Differences between the two patient groups (controls vs. HF patients) were compared with the unpaired Student t-test for continuous variables and the chi-square tests for dichotomous variables. Differences between HF patients with moderate to severe FMR and HF patients without FMR were evaluated with the unpaired Student t-test. In addition, univariate linear regression analysis was performed to correlate various MSCT data on mitral valve geometry (mitral valve tenting height, anterior and posterior leaflet angles, mitral valve sphericity index) with the effective regurgitant orifice area obtained from echocardiography. Subsequently, major determinants of FMR severity were assessed among MSCT data on mitral valve geometry with a significant correlation in the univariate analysis (p<0.05). For this purpose, multivariate linear regression analysis based on enter multiple regression analysis was performed. The dependent variable was the effective orifice regurgitant area and independent variables were anterior and posterior mitral leaflet angles and mitral tenting height at antero-lateral, central and posteromedial levels and the mitral valve sphericity index.

The reproducibility for the assessment of the tenting height, posterior and anterior leaflet angle at each level of the mitral valve was analyzed with repeated measurements by one experienced observer at two different time points and by a second experienced observer. Intra- and inter-observer agreements for these measurements were evaluated by Bland-Altman analysis. Furthermore, intra-class correlation coefficients were used as indicators of reproducibility.

All statistical analyses were performed with SPSS software (version 12.0, SPSS Inc., Chicago, Illinois). All statistical tests were two-sided, and a p-value <0.05 was considered statistically significant.

RESULTS

Study population

A total of 151 patients (mean age 60 ± 11, 87 men) were studied. The overall population was divided into two groups: controls (n = 84) and HF patients (n = 67; 36 [54%] with ischemic cardiomyopathy and 31 [46%] with idiopathic cardiomyopathy). Baseline characteristics of the two groups are shown in Table 2.

Anatomic variations of subvalvular apparatus

In the majority of the patients, the anterior PM had a single insertion in the LV wall, either with 1 PM head (type I, n = 75 [50%]) or 2 PM heads (type IIA n = 49 [33%]). Other anatomical variations of the anterior PM are listed in Table 3. In contrast, the anatomy of the posterior PM was more variable, showing multiple PM heads or multiple PM insertions in the majority of the patients (Table 3).

Table 2. Baseline characteristics of the study population

	Controls (n = 84)	HF patients (n = 67)
Age (yrs)	57 ± 11	63 ± 11 *
Gender (M/F)	47/37	40/27
Body surface area (m^2)	1.9 ± 0.2	1.9 ± 0.2
Hypertension, n (%)	37 (44)	29 (43)
Hypercholesterolemia, n (%)	32 (38)	27 (40)
Diabetes mellitus, n (%)	29 (35)	15 (22)
Smoking, n (%)	24 (29)	27 (40)
Positive family history, n (%)	25 (30)	24 (36)
Previous myocardial infarction, n (%)	0	23 (34)
Anterior location, n(%)	0	14 (23)
Inferior location, n(%)	0	9 (14)
MR severity, n (%)		
Non-MR	54 (64)	4 (6)
Mild	30(36)	44(51)
Moderate	0	14 (21)
Severe	0	15 (22)

*p-value = 0.002; HF = heart failure; MR = mitral regurgitation.

Table 3. Anatomic variations of the papillary muscles (n=151)

Type	Anterior PM	Posterior PM
I	75 (50%)	31 (21%)
IIA	49 (33%)	43 (29%)
IIB	15 (10%)	48 (32%)
IIIA	8 (5%)	6 (4%)
IIIB	4 (3%)	14 (9%)
IIIC	0	9 (6%)

PM = papillary muscle.

In addition, the type of attachment of the PMs to the LV wall was assessed. In all patients the solid body of the PM connected to the solid portion of the LV wall through a network of trabeculae covering the surface of the LV cavity. This type of attachment was seen for both the anterior PM and the posterior PM in all patients.

Left ventricular and mitral valve geometry

The HF patients showed significantly larger LV volumes and lower LVEF as compared to controls (Table 4). In addition, the LV sphericity index was significantly increased in the HF patients (0.4 ± 0.1 vs. 0.3 ± 0.1; p<0.001). The area of the mitral annulus was significantly higher in HF patients compared to controls (Table 4), indicating annular dilatation. In addition, both the AP diameter and the CC diameter of the mitral annulus were increased in the HF patients.

Table 4. Left ventricular and mitral valve geometry in the study population

	Controls (n=84)	HF patients (n=67)	p-value
LVEDV index (ml/m^2)	63 ± 15	95 ± 33	<0.0001
LVESV index (ml/m^2)	23 ± 9	66 ± 31	<0.0001
LVEF (%)	62 ± 13	33 ± 12	<0.001
LV Sphericity index	0.3 ± 0.1	0.4 ± 0.1	<0.001
Mitral annulus area index (cm^2/m^2)	4.8 ± 0.9	5.8 ± 1.4	<0.0001
CC-D index (mm/m^2)	21.6 ± 2.5	23.6 ± 2.9	<0.0001
AP-D index (mm/m^2)	12.5 ± 2.1	15.0 ± 2.7	<0.0001
Mitral valve sphericity index	1.2 ± 0.2	1.3 ± 0.3	0.02
D-PM index (mm/m^2)	11.3 ± 2.4	15.4 ± 2.8	<0.0001
Aα (°)			
Anterolateral	24.6 ± 8.1	29.8 ± 9.6	<0.001
Central	24.6 ± 7.0	32.2 ± 9.8	<0.001
Posteromedial	23.6 ± 7.6	28.6 ± 10.0	0.001
Pα (°)			
Anterolateral	27.1 ± 8.6	30.7 ± 10.3	0.02
Central	34.7 ± 9.6	40.3 ± 10.9	0.001
Posteromedial	28.4 ± 8.7	32.8 ± 10.5	0.006
MVTHt index (mm/m^2)			
Anterolateral	3.4 ± 0.9	4.5 ± 1.2	<0.0001
Central	4.2 ± 1.1	5.8 ± 1.5	<0.0001
Posteromedial	3.4 ± 0.9	4.6 ± 1.5	<0.0001

AP-D = mitral valve anteroposterior diameter; Aα = anterior leaflet angle; CC-D = mitral valve intercommissural diameter; D-PM = distance between the heads of the papillary muscles; HF = heart failure; LVEDV = left ventricular end-diastolic volume index; LVEF = left ventricular ejection fraction; LVESV = left ventricular end-systolic volume index; MVTHt = mitral valve tenting height; Pα = posterior leaflet angle.

The mitral valve sphericity index was defined as the ratio between the distance at the level of the basis of the PMs and the distance between this level and the mitral annulus plane (Figure 5). In the HF patients, a significantly greater distance between the bases of the PMs was observed (15.4 ± 1.8 mm/m^2 vs. 11.3 ± 2.4 mm/m^2; p<0.001). In addition, the distance between the mitral annulus level and the PM line was significantly different (24.9 ± 4.3 mm/m^2 vs. 22.3 ± 3.6 mm/m^2; p<0.0001). As a consequence, the mitral valve sphericity index was significantly larger in HF patients (Table 4). In addition, the distance between the heads of the PMs was also significantly larger in HF patients (Table 4). Finally, HF patients showed a significant increase in the leaflet angles with a significantly higher tenting height at all 3 levels of the mitral valve (Table 4).

Mitral valve geometry in patients with FMR

Among HF patients, 29 patients showed on echocardiography moderate to severe FMR (mean regurgitant volume 64.6 ± 21.8 ml/beat and mean effective regurgitant orifice area 0.4 ± 0.1 cm^2). To detect changes in mitral valve geometry in FMR, HF patients with moderate to severe FMR (n=29) were compared with HF patients without FMR (n=38). Previous history of inferior myocardial infarction was present in 2 (7%) HF patients with moderate to severe FMR and in 7 (18%) HF patients without (p = 0.11). The patients with moderate to severe FMR had comparable LV volumes and LVEF to patients without FMR (Table 5). The mitral annulus area was significantly larger among patients with moderate to severe FMR, with also a significantly larger CC diameter (Table 5).

The distance between the basis of the PMs was larger in HF patients with moderate to severe FMR as compared to HF patients without FMR (16.5 ± 2.6 mm/m^2 vs. 14.7 ± 2.7 mm/m^2, respectively; p=0.006). There were no differences in the distance between the PM line and the mitral annulus plane between both groups of patients (25.1 ± 3.5 mm/m^2 vs. 24.8 ± 4.9 mm/m^2; p=0.8). Consequently, the sphericity index of the mitral valve was significantly higher in HF patients with moderate to severe FMR (Table 5). In addition, the distance between the heads of the PMs was significantly larger among HF patients with moderate to severe FMR (Table 5).

Compared to HF patients without FMR, HF patients with moderate to severe FMR showed an asymmetrical deformation of the mitral valve. Particularly, the angles of the posterior leaflet values at central and posteromedial levels were significantly higher, whereas no significant differences were observed either at the anterolateral level or the angles of the anterior leaflet (Table 5). As a consequence, the differences in mitral valve tenting height were more prominent at the central and the posteromedial levels (Table 5).

MSCT determinants of FMR severity

All MSCT derived parameters on mitral valve geometry (mitral valve tenting height, anterior and posterior leaflet angles and mitral valve sphericity index) showed a significant correlation with the effective regurgitant orifice area assessed by echocardiography in all 3 levels of the mitral valve (anterolateral, central and posteromedial) (Table 6). However, on multivariate

analysis, the mitral valve tenting height at the central level (r = 0.58; p<0.0001) and the mitral valve sphericity index (r = 0.36; p<0.0001) were the strongest determinants of FMR severity.

Table 5. Left ventricular and mitral valve geometry in HF patients with and without moderate to severe FMR

	HF patients with moderate to severe FMR (n=29)	HF patients without FMR (n=38)	p-value
EROA (cm^2)	0.4 ± 0.1	0.1 ± 0.02	<0.0001
Regurgitant volume (ml/beat)	64.6 ± 21.8	15.6 ± 12.3	<0.0001
LVEDV index (ml/m^2)	101 ± 37	91 ± 30	0.2
LVESV index (ml/m^2)	72 ± 37	62 ± 25	0.2
LVEF (%)	32 ± 14	33 ± 10	0.7
LV Sphericity index	0.4 ± 0.1	0.3 ± 0.1	0.1
Mitral annulus area index (cm^2/m^2)	6.3 ± 1.7	5.4 ± 0.9	0.02
CC-D index (mm/m^2)	24.8 ± 2.5	22.8 ± 2.9	0.006
AP-D index (mm/m^2)	15.6 ± 2.9	14.5 ± 2.4	0.1
Mitral valve sphericity index	1.4 ± 0.3	1.2 ± 0.3	0.004
D-PM index (mm/m^2)	16.5 ± 2.5	14.7 ± 2.7	0.006
Aα (°)			
Anterolateral	29.9 ± 8.3	29.9 ± 10.6	0.9
Central	33.2 ± 8.6	31.5 ± 10.7	0.5
Posteromedial	30.9 ± 9.7	26.8 ± 10.1	0.1
Pα (°)			
Anterolateral	32.3 ± 10.9	29.5 ± 9.7	0.3
Central	44.4 ± 11.9	37.1 ± 9.0	0.008
Posteromedial	35.9 ± 10.6	26.8 ± 10.1	0.04
MVTHt index (mm/m^2)			
Anterolateral	4.8 ± 1.2	4.2 ± 1.0	0.02
Central	6.6 ± 1.4	5.3 ± 1.3	<0.0001
Posteromedial	5.4 ± 1.6	4.1 ± 1.2	<0.0001

EROA = effective regurgitant orifice area; FMR = functional mitral regurgitation; other abbreviations as in Table 4.

Table 6. MSCT determinants of effective regurgitant orifice area: univariate and multivariate analysis.

	Univariate		Multivariate
	r	p-value	p-value
Aα (°)			
Anterolateral	0.19	0.02	0.7
Central	0.31	<0.0001	0.3
Posteromedial	0.26	0.001	…
Pα (°)			
Anterolateral	0.25	0.002	0.3
Central	0.32	<0.0001	0.9
Posteromedial	0.25	0.002	…
MVTHt index (mm/m^2)			
Anterolateral	0.36	<0.0001	0.5
Central	0.53	<0.0001	<0.0001
Posteromedial	0.43	<0.0001	…
Mitral valve sphericity index	0.36	<0.0001	<0.0001

R^2 of the model selected for multivariate analysis = 0.428. The anterior and posterior leaflet angle and the mitral valve tenting height at the posteromedial level were not included in the model because of the high inter-correlation of these variables (Pearson correlation coefficient >0.70). Aα = anterior leaflet angle; MVTHt = mitral valve tenting height; Pα = posterior leaflet angle.

Reproducibility data

In 15 randomly selected patients, reproducibility data was assessed. The intra-observer agreement for the tenting height and leaflet angle measurements was good. The average differences were: 0.9 ± 1.4% for the tenting height, -3.3 ± 5.7% for the posterior leaflet angle, and -0.8 ± 4.9% for the anterior leaflet angle. The intra-class correlation coefficients for each intra-observer comparison were: 0.92 for the tenting height, 0.86 for the posterior leaflet angle and 0.85 for the anterior leaflet angle.

Similarly, agreement of the measurements by two different observers was good. The average differences were: 0.1 ± 1.2% for the tenting height, 0.9 ± 2.9% for the posterior leaflet angle and -0.4 ± 4.4% for the anterior leaflet angle. The intra-class correlation coefficients for each inter-observer comparison were: 0.84 for the tenting height, 0.83 for the posterior leaflet angle and 0.84 for the anterior leaflet angle.

DISCUSSION

The present study demonstrates that MSCT enables a comprehensive assessment of the mitral valve apparatus, by providing an exact characterization of the anatomy of the subvalvular apparatus and the geometry of the mitral valve. The main findings can be summarized as follows: the anatomy of the subvalvular apparatus is highly variable, with variations in both the number of heads and insertions of the anterior and posterior PMs. Furthermore, the attachment of the PMs to the LV wall is not solid, but trabecularized in all patients. With the use of MSCT, an asymmetric deformation of the mitral valve was observed in HF patients with moderate to severe FMR. The posterior leaflet angles and the mitral valve tenting height were significantly increased at the central and the posteromedial levels, as compared to HF patients without FMR. In addition, a more outward displacement of the PMs, reflected by a higher mitral valve sphericity index, was observed in this subgroup of patients. The findings of the present study may have important implications for surgical mitral valve repair in patients with severe FMR.

Anatomic variations of subvalvular apparatus

A large variability in the anatomy of the subvalvular apparatus was observed in the present study (Figure 1 and Table 3). The characterization of the subvalvular apparatus may be of great importance for various surgical mitral valve repair approaches that include translocation or reconstruction and relocation of the PMs (11,17). Previous anatomical studies have also reported variations in PM anatomy (13,18). Berdajs et al. (13) studied 100 structural normal hearts and classified the PMs according to the number of heads and insertions (Figure 1). The authors demonstrated that the anatomy of the posterior PM was more heterogeneous compared with the anterior PM (13). The results of the present study are in line with previous anatomical studies: in

the majority of the patients, the posterior PM consisted of multiple heads or multiple insertions, whereas the anatomy of the anterior PM was more homogeneous (Table 3).

In addition to PM anatomy, the characteristics of the PM attachments to the LV wall were assessed in the present study. Conventionally, the anchorage of the PM to the solid heart wall has been described as a direct connection with a broad base. However, recently, Axel noted that the attachment may rather be through a network of trabeculae (19). In the present study, similar attachments of the PMs were found. In all patients the bases of the PMs connected to the solid wall of the LV through a network of trabeculae instead of a solid attachment (Figure 1). The attachment of the PMs to the LV wall may have implications for surgical mitral valve repair. However, the exact clinical importance of this finding remains to be determined. Nonetheless, MSCT allows for a detailed analysis of the anatomy of the PMs and their attachment to the LV wall.

Geometric changes in FMR

The geometry of the mitral valve was studied in 29 HF patients with moderate to severe FMR, and compared to HF patients without FMR (n = 38). In HF patients with moderate to severe FMR, remodeling of the LV and the mitral valve was observed. Importantly, mitral valve deformation affected predominantly the central and posteromedial parts of the valve, and the increase in mitral valve tenting height at the central level was the strongest determinant of FMR severity. In addition, the higher sphericity index of the mitral valve indicates that the displacement of the PMs plays a role in the development of FMR. These results are in agreement with previous in vitro and in vivo studies (9,20). Nielsen et al. (20) used an in vitro LV model to study the impact of PM misalignment on mitral leaflet coaptation and its relation with the severity of mitral regurgitation. The asymmetrical displacement of the PMs towards a more posterior level resulted in preserved or excessive anterior leaflet motion (prolapse-like) at the anterolateral level (close to the anterior commissure), whereas at the posteromedial level (close to the posterior commissure), a failure of leaflet coaptation was observed (20). Kwan et al. (9), confirmed these results using 3-dimensional echocardiography in patients with ischemic cardiomyopathy. An asymmetrical deformation of the mitral valve, with a "funnel-shaped" deformity on the level close to the posterior commissure and a "prolapse-like" deformity on the anterolateral side, was noted in patients with ischemic cardiomyopathy, in contrast to patients with idiopathic cardiomyopathy (9). The present study confirms these results and demonstrates that MSCT may be of value for assessment of mitral valve remodeling in patients with FMR.

Determinants of FMR severity

The geometry parameters of the mitral valve assessed by 64-slice MSCT were related to the severity of FMR, particularly the mitral valve tenting height at the central level and the sphericity index of the mitral valve. These findings are in agreement with previous data based on 2- and 3-dimensional echocardiography (9). Kwan et al. demonstrated using 3-dimensional

echocardiography, that the medial mitral valve tenting area was the major determinant of the severity of mitral regurgitation in patients with dilated cardiomyopathy (9). In addition, the mitral valve sphericity index, as an indicator of the outward displacement of the PMs, suggests that FMR severity is also related to changes in LV cavity geometry, as previously described (21).

Clinical implications

Accurate assessment of the interaction of the LV and the mitral valve apparatus is crucial in surgical treatment of FMR (8). New surgical techniques that include restoration of LV geometry and relocation of the PMs have been proposed (11,17). For these procedures, an exact characterization of the LV geometry and the subvalvular apparatus is mandatory. Furthermore, assessment of the deformation of the mitral annulus is important for surgical procedures that attempt to restore the geometry of the mitral valve (12). Finally, the assessment of leaflet tethering is of critical importance and may even predict the outcome of surgical mitral valve repair (22).

Previously, it has been demonstrated that MSCT may be of value for assessment of mitral valve anatomy (23-25). However, in none of these studies, the geometry of the mitral valve and the interaction with the LV was studied. In the present study, 64-slice MSCT was used to assess mitral valve anatomy and geometry in a large cohort of patients, including patients with FMR. By providing detailed information on all components of the LV and mitral valve complex, MSCT may be of great value to guide surgical therapy for FMR.

Study limitations

There is little evidence on the assessment of regurgitant mitral valve with MSCT (26). In the present study, the regurgitant orifice area was not quantified with MSCT, which is a limitation. Furthermore, surgical data was not systematically available in all patients with FMR, precluding us to confirm prospectively the value of MSCT in the surgical treatment decision. Future studies, assessing both the anatomical and the functional aspects of the mitral valve with MSCT and with larger populations including patients with several grades of FMR, may provide more insight in this issue. Finally, radiation dose (currently 10-15 mSv) is one of the general disadvantages of MSCT and adjustments in imaging protocols are warranted to keep the radiation exposure within limits.

CONCLUSIONS

The present study shows that MSCT allows detailed assessment of mitral valve anatomy and geometry. In patients with moderate to severe FMR, an asymmetrical remodeling of the mitral valve was observed, with tethering of the mitral leaflets at the central and posteromedial levels of the mitral valve. MSCT provides the anatomical and geometric analysis of the mitral valve apparatus and may be of value to guide surgical treatment of FMR.

REFERENCES

1. Feinberg MS, Schwammenthal E, Shlizerman L et al. Prognostic significance of mild mitral regurgitation by color Doppler echocardiography in acute myocardial infarction. Am J Cardiol 2000;86:903-7.

2. Grigioni F, Enriquez-Sarano M, Zehr KJ, Bailey KR, Tajik AJ. Ischemic mitral regurgitation: long-term outcome and prognostic implications with quantitative Doppler assessment. Circulation 2001;103:1759-64.

3. Koelling TM, Aaronson KD, Cody RJ, Bach DS, Armstrong WF. Prognostic significance of mitral regurgitation and tricuspid regurgitation in patients with left ventricular systolic dysfunction. Am Heart J 2002;144:524-9.

4. Borger MA, Alam A, Murphy PM, Doenst T, David TE. Chronic ischemic mitral regurgitation: repair, replace or rethink? Ann Thorac Surg 2006;81:1153-61.

5. Calafiore AM, Gallina S, Di MM et al. Mitral valve procedure in dilated cardiomyopathy: repair or replacement? Ann Thorac Surg 2001;71:1146-52.

6. McGee EC, Gillinov AM, Blackstone EH et al. Recurrent mitral regurgitation after annuloplasty for functional ischemic mitral regurgitation. J Thorac Cardiovasc Surg 2004;128:916-24.

7. Mihaljevic T, Lam BK, Rajeswaran J et al. Impact of mitral valve annuloplasty combined with revascularization in patients with functional ischemic mitral regurgitation. J Am Coll Cardiol 2007;49:2191-201.

8. Levine RA, Schwammenthal E. Ischemic mitral regurgitation on the threshold of a solution: from paradoxes to unifying concepts. Circulation 2005;112:745-58.

9. Kwan J, Shiota T, Agler DA et al. Geometric differences of the mitral apparatus between ischemic and dilated cardiomyopathy with significant mitral regurgitation: real-time three-dimensional echocardiography study. Circulation 2003;107:1135-40.

10. Yu HY, Su MY, Liao TY, Peng HH, Lin FY, Tseng WY. Functional mitral regurgitation in chronic ischemic coronary artery disease: analysis of geometric alterations of mitral apparatus with magnetic resonance imaging. J Thorac Cardiovasc Surg 2004;128:543-51.

11. Liel-Cohen N, Guerrero JL, Otsuji Y et al. Design of a new surgical approach for ventricular remodeling to relieve ischemic mitral regurgitation: insights from 3-dimensional echocardiography. Circulation 2000;101:2756-63.

12. Gillinov AM, Cosgrove DM, III, Shiota T et al. Cosgrove-Edwards Annuloplasty System: midterm results. Ann Thorac Surg 2000;69:717-21.

13. Berdajs D, Lajos P, Turina MI. A new classification of the mitral papillary muscle. Med Sci Monit 2005;11:BR18-21.

14. Kono T, Sabbah HN, Stein PD, Brymer JF, Khaja F. Left ventricular shape as a determinant of functional mitral regurgitation in patients with severe heart failure secondary to either coronary artery disease or idiopathic dilated cardiomyopathy. Am J Cardiol 1991;68:355-9.

15. Schiller NB, Shah PM, Crawford M et al. Recommendations for quantitation of the left ventricle by two-dimensional echocardiography. J Am Soc Echocardiogr 1989;2:358-67.

16. Bonow RO, Carabello BA, Kanu C et al. ACC/AHA 2006 guidelines for the management of patients with valvular heart disease. Circulation 2006;114:e84-231.

17. Kron IL, Green GR, Cope JT. Surgical relocation of the posterior papillary muscle in chronic ischemic mitral regurgitation. Ann Thorac Surg 2002;74:600-1.

18. Victor S, Nayak VM. Variations in the papillary muscles of the normal mitral valve and their surgical relevance. J Card Surg 1995;10:597-607.

19. Axel L. Papillary muscles do not attach directly to the solid heart wall. Circulation 2004;109:3145-8.

20. Nielsen SL, Nygaard H, Fontaine AA et al. Papillary muscle misalignment causes multiple mitral regurgitant jets: an ambiguous mechanism for functional mitral regurgitation. J Heart Valve Dis 1999;8:551-64.

21. Yiu SF, Enriquez-Sarano M, Tribouilloy C, Seward JB, Tajik AJ. Determinants of the degree of functional mitral regurgitation in patients with systolic left ventricular dysfunction: A quantitative clinical study. Circulation 2000;102:1400-6.

22. Magne J, Pibarot P, Dagenais F, Hachicha Z, Dumesnil JG, Senechal M. Preoperative posterior leaflet angle accurately predicts outcome after restrictive mitral valve annuloplasty for ischemic mitral regurgitation. Circulation 2007;115:782-91.

23. Willmann JK, Kobza R, Roos JE et al. ECG-gated multi-detector row CT for assessment of mitral valve disease: initial experience. Eur Radiol 2002;12:2662-9.

24. Alkadhi H, Bettex D, Wildermuth S et al. Dynamic cine imaging of the mitral valve with 16-MDCT: a feasibility study. AJR Am J Roentgenol 2005;185:636-46.

25. Messika-Zeitoun D, Serfaty JM, Laissy JP et al. Assessment of the mitral valve area in patients with mitral stenosis by multislice computed tomography. J Am Coll Cardiol 2006;48:411-3.

26. Alkadhi H, Wildermuth S, Bettex DA et al. Mitral regurgitation: quantification with 16-detector row CT--initial experience. Radiology 2006;238:454-63.